JACS
JOURNAL OF THE AMERICAN CHEMICAL SOCIETY
Communication
pubs.acs.org/JACS

Molecular Design toward Efficient Polymer Solar Cells with High Polymer Content

Deping Qian,[†,§] Wei Ma,[*,‡] Zhaojun Li,[†] Xia Guo,[†] Shaoqing Zhang,[†] Long Ye,[†] Harald Ade,[‡] Zhan'ao Tan,[*,§] and Jianhui Hou[*,†]

[†]State Key Laboratory of Polymer Physics and Chemistry, Beijing National Laboratory for Molecular Sciences, Institute of Chemistry, Chinese Academy of Sciences, Beijing 100190, China

[‡]Department of Physics, North Carolina State University, Raleigh, North Carolina 27695, United States

[§]The New and Renewable Energy of Beijing Key Laboratory, School of Renewable Energy, North China Electric Power University, Beijing 102206, China

Supporting Information

ABSTRACT: A novel polythiophene derivative, PBT1, was designed, synthesized, and applied in polymer solar cells (PSCs). This work provides a successful example of using molecular structure as a tool to realize optimal photovoltaic performance with high polymer content, thus enabling the realization of efficient photoabsorption in very thin films. As a result, an efficiency of 6.88% was recorded in a PSC with a 75 nm active layer.

Polymer solar cells (PSCs) with bulk heterojunction (BHJ) structure are particularly attractive because of their ease of processing, large area with mechanical flexibility, and potential low-cost production.[1] The typical BHJ layer in PSCs is composed of a blend of two ingredients, a polymer as the electron donor and a polymer or small-molecule compound as the electron acceptor. Great effort has been devoted to modulating the properties of the BHJ layers, which strongly advanced the field in the past decade. In general, the molecular design of active-layer materials and morphology control of the BHJ blends are the two mainly adopted approaches for improving the photovoltaic performance of PSC devices. Several molecular design strategies have been successfully used to modulate absorption spectra,[2,3] band gaps,[2,3] and molecular energy levels[2,3] of the active-layer materials, resulting in significant improvements in the photovoltaic performance of PSC devices.[4] In these reported works, PCBM[5] [an abbreviation denoting two fullerene derivatives, phenyl-C_{61}-butyric acid methyl ester ($PC_{61}BM$) and phenyl-C_{71}-butyric acid methyl ester ($PC_{71}BM$)] was primarily used as the electron acceptor in the BHJ blends. The optimal polymer/PCBM composition in the blends is generally polymer-deficient and varies from 50% to 80%, corresponding to donor/acceptor (D/A) weight ratios of 1:1 to 1:4 for a range of polymers used as donor materials.[6−9]

As is well-known, $PC_{61}BM$ and $PC_{71}BM$ show weaker extinction coefficients and narrower absorption bands than low-band-gap conjugated polymers. Reducing the feed ratio of PCBM in the blend would thus be helpful to harvest more sunlight from the blend film with limited thickness (i.e., <100 nm). The use of thicker films is often unsuccessful because of increased recombination and degradation of the fill factor (FF).[10] Therefore, to get efficient PSCs with low PCBM content and high polymer content in the blend is an important topic for molecular design. According to the thousands of works in the field of PSCs, an interesting phenomenon can be observed: for a specified polymer/PCBM photovoltaic system, the optimal D/A ratio is almost constant even if much different device fabrication processes and/or device structures are employed. For example, different strategies have been used to optimize the morphology of the poly(3-hexylthiophene) (P3HT)/PCBM blend to improve its photovoltaic performance,[9,11,12] but the optimal D/A ratios used in these works are all ∼1:1. This interesting phenomenon can also be confirmed for most other polymer/PCBM photovoltaic systems, including PSBTBT/PCBM,[13] PCDTBT/PCBM,[14] PBDTTT/PCBM,[4] and so on. Therefore, it seems that the optimal D/A ratio of a blend should be correlated with one of the intrinsic properties determined by the polymer's molecular structure. Therefore, it is very interesting and also important to use molecular structure as a tool to realize efficient photovoltaic performance with low $PC_{71}BM$ content and high polymer content.

Recently, interesting reported results have demonstrated that under certain conditions PCBM can intercalate into the space between the adjacent side chains of the polymer, and therefore, a significant excess of PCBM is needed to get bicontinuous phase separation.[15] For example, the distance between the adjacent alkyl side groups of PBTTT is larger than the diameter of a PCBM molecule, allowing intercalation of PCBM molecules to take place, and therefore, the optimal device performance was obtained at a D/A ratio of 1:4.[15] According to these results, it seems that the alkyl side groups play an important role in modulating the D/A ratio in polymer/PCBM blends. Therefore, in this work we modified the substituent position of the alkyl chains in a polythiophene derivative, PBT1 (Scheme 1), to realize efficient PSCs with high D/A ratio.

As a polythiophene derivative, PBT1 has a backbone consisting of repeating benzodithiophene-4,8-dione and α-quaterthiophene units in which π electrons can be delocalized effectively through the alternative electron push−pull effect,

Received: March 24, 2013
Published: May 24, 2013

 © 2013 American Chemical Society dx.doi.org/10.1021/ja402971d | J. Am. Chem. Soc. 2013, 135, 8464−8467

Scheme 1. Molecular Structure and Synthesis of PBT1[a]

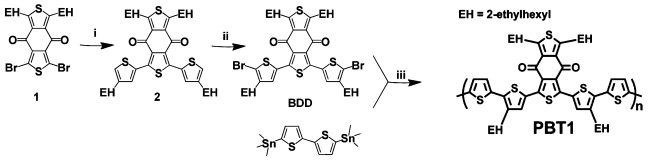

[a]Conditions: (i) 2-Tributylstannyl-4-(2-ethylhexyl)thiophene, Pd(PPh$_3$)$_4$, toluene, reflux, 12 h. (ii) NBS, chloroform, ambient temperature, 12 h; Pd(PPh$_3$)$_4$, toluene, reflux, 16 h.

allowing a low band gap to be realized. The synthesis of PBT1 is shown in Scheme 1, and the detailed synthetic procedures are provided in the Supporting Information (SI). The benzo[1,2-*c*:4,5-*c*′]dithiophene-4,8-dione monomer was prepared by the reported method.[16] The polymer was prepared by a Stille polycondensation reaction in ∼80% yield. The number-average molecular weight (M_n) and polydispersity (PDI) of the polymers were 38 kDa and 2.12, respectively, as estimated by gel-permeation chromatography (GPC) using monodispersed polystyrene as the standard and chloroform as the eluent. The polymers exhibited excellent solubility in chloroform, chlorobenzene, and *o*-dichlorobenzene (*o*-DCB).

The UV−vis absorption spectra of the polymer in chloroform solution and as a solid film are shown in Figure 1a. In

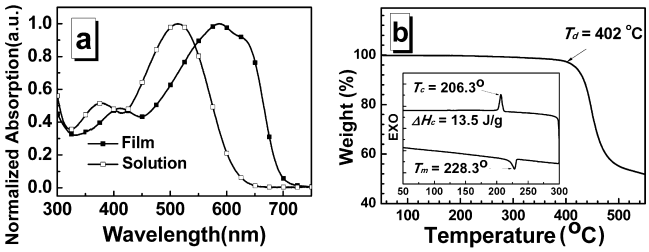

Figure 1. (a) UV−vis absorption spectra of PBT1 in chloroform solution and as a solid film. (b) TGA and (inset) DSC plots for PBT1 under an inert atmosphere at a scan speed of 10 °C/min.

solution, the conjugated backbone of PBT1 may be distorted because of steric hindrance from the bulky 2-ethylhexyl groups, which is overcome by the intermolecular $\pi-\pi$ stacking in the solid state. Therefore, in going from the solution to the solid film, the absorption of PBT1 was distinctly red-shifted (from 512 to 588 nm for the peak and 640 to 700 nm for the absorption edge). Figure S1 in the SI shows the cyclic voltammogram for a PBT1 film on a glassy carbon electrode in acetonitrile containing 0.1 mol/L Bu_4NPF_6. The onset oxidation and reduction potentials are at 0.41 and −1.49 V, respectively, corresponding to a HOMO level of −5.13 eV and a LUMO level of −3.23 eV.[17,18] As shown in Figure 1b, the polymer exhibited a decomposition temperature (T_d) of 402 °C in thermogravimetric analysis (TGA). In differential scanning calorimetry (DSC) analysis, the polymer showed a melting temperature (T_m) of 228.3 °C and a crystallization temperature (T_c) of 206.3 °C. The crystallization enthalpy of the polymer was found to be 13.5 J/g, which is similar to that of regioregular P3HT (rr-P3HT) (Figure S2). The relatively high crystallization enthalpy implies that the attractive intermolecular interactions in PBT1 might be quite strong, which in turn suggests a relatively pure polymer phase in the devices that is simply disordered, as shown below.

PSC devices were fabricated to investigate the photovoltaic properties of the new polymer. The device structure used in this work was ITO/PEDOT:PSS (30 nm)/polymer:PC$_{71}$BM (74−180 nm)/Ca (20 nm)/Al (80 nm); the active layers of the devices were spin-coated from 10 mg/mL solutions in *o*-DCB. It has been well-recognized that the addition of a certain amount of 1,8-diiodooctane (DIO) may be helpful in optimizing the nanoscale morphology of the blends,[19−21] and therefore, different ratios of DIO were used here to optimize the photovoltaic performance. Eventually, when 1% (v/v) DIO/*o*-DCB was used, the devices exhibited enhanced photovoltaic performance (Table S1 in the SI). Since the influence of the addition of DIO has been well-studied, we will not further discuss this issue here.

The *J*−*V* curves for PBT1:PC$_{71}$BM devices with different D/A ratios are shown in Figure S3, and the key photovoltaic parameters are listed in Table 1; the external quantum

Table 1. Photovoltaic Parameters for PBT1-Based PSCs Processed with 1% DIO/*o*-DCB at Different PC$_{71}$BM Feed Ratios

PC71BM content (%)	D/A ratio	thickness (nm)	J_{sc} (mA/cm^2)	V_{oc} (V)	FF	PCE (%)
0	1:0	57	0.05	0.95	0.41	0.02
10	9:1	74	5.27	0.94	0.41	2.03
20	4:1	77	9.85	0.86	0.65	5.44
30	2.33:1	86	10.53	0.83	0.70	6.11
40	1.5:1	75	11.57	0.83	0.71	6.88
50	1:1	83	10.98	0.82	0.71	6.41
60	1:1.5	87	10.01	0.81	0.69	5.60
70	1:2.33	124	7.04	0.81	0.71	4.06
80	1:4	137	6.94	0.80	0.68	3.81
90	1:9	180	2.21	0.81	0.66	1.19

efficiency (EQE) curves and optical densities of the corresponding devices are shown in Figure 2a,b, respectively.

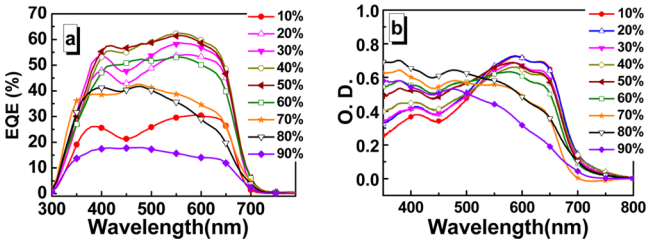

Figure 2. (a) EQE curves for PBT1-based PSCs with different PC$_{71}$BM contents. (b) Optical densities of the active layers of these devices.

When 10% PC$_{71}$BM was used, although the blend film showed strong absorption, the device showed a relatively low EQE over the whole response range, and as a result, the short-circuit current density (J_{sc}) was only 5.27 mA/cm^2. In addition, this device showed a relatively poor FF of 0.41). When the content of PC$_{71}$BM was increased to 20%, the EQE of the device improved significantly, and consequently, the J_{sc} of the device increased to 9.85 mA/cm^2; meanwhile, the FF of the device reached 0.65. When the PC$_{71}$BM content was increased to 30% and then to 40%, both the J_{sc} and FF of the devices improved slightly, and therefore, the power conversion efficiency (PCE) of the device reached 6.88%. When the PC$_{71}$BM content was increased further, the absorbance at 550−700 nm obviously

dx.doi.org/10.1021/ja402971d | J. Am. Chem. Soc. 2013, 135, 8464−8467

dropped because $PC_{71}BM$ has a smaller extinction coefficient than PBT1 in this wavelength range; as a result, the EQE and hence the J_{sc} of the devices decreased gradually. According to the data in Table 1, both J_{sc} and FF for the device with 20% $PC_{71}BM$ are close to the corresponding values for the champion device (the device with 40% $PC_{71}BM$), implying that bicontinuous phase separation with the appropriate domain size may have occurred in this low-PCBM-content device in the presence of DIO, which affords efficient exciton diffusion and charge separation as well as balanced hole and electron transport.[22−25] Finally, it is noteworthy that the mismatch between the integral values and the J_{sc} values obtained from the $J-V$ measurements are within 5%, indicating that the $J-V$ measurements in this work are reliable.

The bulk and surface morphological properties of the D/A blends with different $PC_{71}BM$ contents were investigated by transmission electron microscopy (TEM) and tapping-mode atomic force microscopy (AFM). To demonstrate the evolution of the phase-separated morphology of the blends, the blend films with 10%, 20%, 40% and 90% $PC_{71}BM$ (processed with *o*-DCB and DIO) were characterized in parallel. As we can see in Figure 3a, the blend with 10% $PC_{71}BM$ showed large size

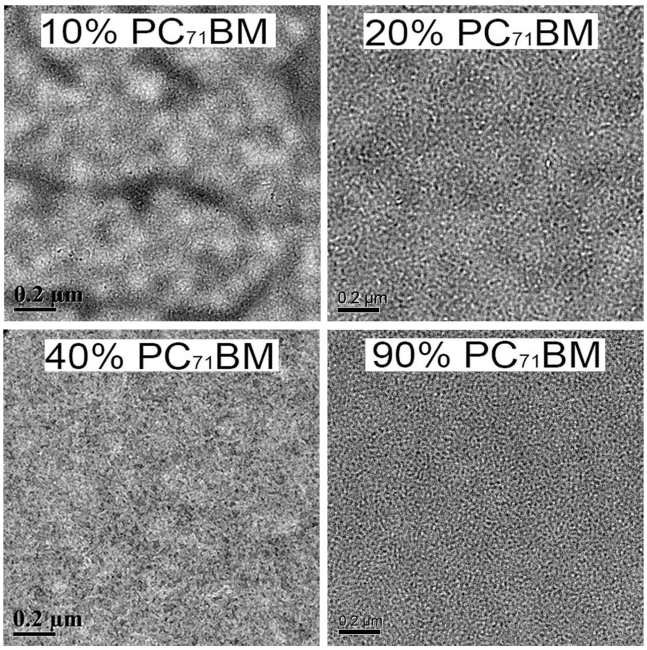

Figure 3. TEM images of PBT1:$PC_{71}BM$ blend films with $PC_{71}BM$ contents of 10%, 20%, 40%, and 90%.

aggregations; the light domains should be ascribed to aggregations of the polymer, and the dark domains should be due to $PC_{71}BM$. When the $PC_{71}BM$ content was increased to 20%, 40%, and 90%, the severe phase separation disappeared, and the TEM images looked quite uniform (Figure 3b−d).

AFM images of the blends and the pure polymer are shown in Figure S4. Interestingly, small granular aggregations with diameters of tens of nanometers were formed in the pure polymer film, and the film was very smooth [root-mean-square roughness (R_q) = 0.75 nm]. In the blend films with 10%, 20% and 40% $PC_{71}BM$, similar-sized aggregations were observed, while the roughness of the films increased to 3 ± 1 nm. According to the phase images, the phase difference in the blend films was slightly higher than that in the pure polymer film, indicating that the polymer phase may have a similar modulus as $PC_{71}BM$ phase.

To investigate the polymer crystallinity and lamellar spacing, we analyzed grazing-incidence X-ray diffraction (GIXD) profiles of the blend film in the optimal PSC device (i.e., 40% $PC_{71}BM$) and the pure PBT1 film (Figure 4). The GIXD

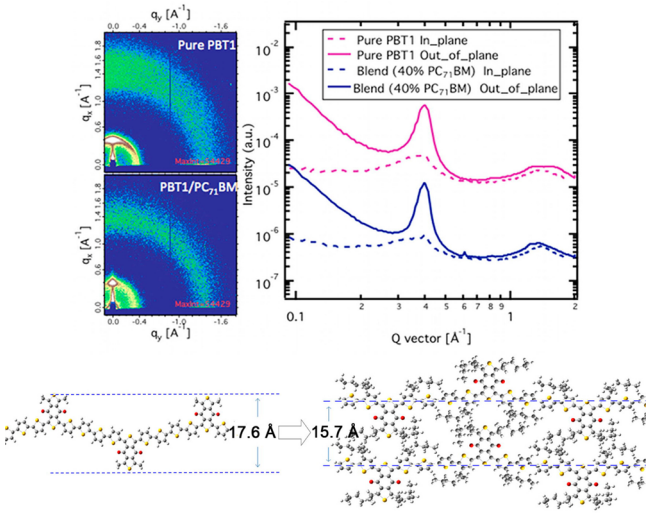

Figure 4. GIXD profiles of the pure PBT1 film and the blend film with 40% $PC_{71}BM$. The illustration at the bottom demonstrates the width of the rigid segment and the compact interchain packing in PBT1.

profile of the pure PBT1 film showed a clear (100) peak at ~0.40 $Å^{-1}$. When PBT1 was blended with $PC_{71}BM$, the location of the (100) peak did not shift, which implies that lamellar spacing remained unchanged (unlike the case of PBTTT).[15] We note that the (100) peak of PBT1 at 0.40 $Å^{-1}$ corresponds to a *d* spacing of 15.7 Å. This is a very small lamellar spacing compared with most widely used conjugated polymers, such as P3HT (16.7 Å),[26] PTB7 (17−19 Å),[27] and PCDTBT (>21 Å).[28] According to theoretical simulations, the rigid part of PBT1 shows a width of 17.6 Å (Figure S5), which is larger than the lamellar spacing obtained from the GIXD analysis, indicating that very compact packing may form between the adjacent polymer chains (Figure S5). Obviously, the compact interchain packing should help to improve the intermolecular charge transport in the nonfavorable direction within the polymer domains.

In conclusion, a novel polythiophene derivative, PBT1, was designed, synthesized, and applied in PSCs. Branched alkyl groups were introduced at specific substitution positions to ensure that the lamellar spacing of PBT1 would be smaller than the width of the rigid segments of the polymer, which itself is also smaller than the width of many widely used conjugated polymers. As a result, in the PBT1:$PC_{71}BM$ photovoltaic system, less $PC_{71}BM$ was required in order to get optimal photovoltaic performance. A PCE of 6.88% was observed when 40% $PC_{71}BM$ was used in the blend, corresponding to a D/A ratio of 1.5:1. More interestingly, when 20% $PC_{71}BM$ was employed in the blend, corresponding to a D/A ratio of 4:1, a PCE of 5.42% could still be realized. This work provides the first successful example of the use of molecular structure as a tool to realize efficient photovoltaic performance with high polymer content and low $PC_{71}BM$ content. This opens up a new approach for achieving high absorption in thin active layers in PSCs with good FF and thus high performance. By avoiding

dx.doi.org/10.1021/ja402971d | *J. Am. Chem. Soc.* 2013, 135, 8464−8467

problems with morphology control and recombination that arise with the use of thicker films, the synthesis of materials yielding high-D/A-ratio devices thus leads to an alternate and possibly easier route to optimized performance.

■ ASSOCIATED CONTENT

Ⓢ Supporting Information

Photovoltaic performance based on PBT1:$PC_{71}BM$ obtained with different amounts of DIO; experimental details of the synthesis of the polymer, device fabrication, and characterization of the PSCs; DSC diagram of P3HT for comparison; AFM images of the blend films; and optimized backbone structure of PBT1 simulated by DFT at the B3LYP/6-31G(d,p) level. This material is available free of charge via the Internet at http://pubs.acs.org.

■ AUTHOR INFORMATION

Corresponding Author

hjhzlz@iccas.ac.cn; wma5@ncsu.edu; tanzhanao@ncepu.edu.cn

Notes

The authors declare no competing financial interest.

■ ACKNOWLEDGMENTS

This work was supported by the National Natural Science Foundation of China, the Chinese Academy of Sciences, and The Chinese Ministry of Science and Technology (51173189, KJ2D-EW-J01, 2011DFG63460, 2011AA050523). The X-ray characterization and interpretation by NCSU was supported by the U.S. Department of Energy (DE-FG02-98ER45737).

■ REFERENCES

(1) Yu, G.; Gao, J.; Hummelen, J. C.; Wudl, F.; Heeger, A. J. *Science* **1995**, *270*, 1789.

(2) Hou, J. H.; Park, M.; Zhang, S. Q.; Yao, Y.; Chen, L. M.; Li, J. H.; Yang, Y. *Macromolecules* **2008**, *41*, 6012.

(3) Li, Y. F. *Acc. Chem. Res.* **2012**, *45*, 723.

(4) Chen, H. Y.; Hou, J. H.; Zhang, S. Q.; Liang, Y. Y.; Yang, G. W.; Yang, Y.; Yu, L. P.; Wu, Y.; Li, G. *Nat. Photonics* **2009**, *3*, 649.

(5) Meier, M. S.; Poplawska, M. *J. Org. Chem.* **1993**, *58*, 4524.

(6) Guo, X.; Zhang, M. J.; Tan, J. H.; Zhang, S. Q.; Huo, L. J.; Hu, W. P.; Li, Y. F.; Hou, J. H. *Adv. Mater.* **2012**, *24*, 6536.

(7) Wang, E. G.; Hou, L. T.; Wang, Z. Q.; Hellstrom, S.; Zhang, F. L.; Inganas, O.; Andersson, M. R. *Adv. Mater.* **2010**, *22*, 5240.

(8) Wienk, M. M.; Kroon, J. M.; Verhees, W. J. H.; Knol, J.; Hummelen, J. C.; Van Hal, P. A.; Janssen, R. A. J. *Angew. Chem., Int. Ed.* **2003**, *42*, 3371.

(9) (a) Li, G.; Shrotriya, V.; Huang, J. S.; Yao, Y.; Moriarty, T.; Emery, K.; Yang, Y. *Nat. Mater.* **2005**, *4*, 864. (b) Li, G.; Yao, Y.; Yang, H.; Shrotriya, V.; Yang, G.; Yang, Y. *Adv. Funct. Mater.* **2007**, *17*, 1636. (c) Shi, C. J.; Yao, Y.; Yang, Y.; Pei, Q. B. *J. Am. Chem. Soc.* **2006**, *128*, 8980 .

(10) Bartelt, J. A.; Beiley, Z. M.; Hoke, E. T.; Mateker, W. R.; Douglas, J. D.; Collins, B. A.; Tumbleston, J. R.; Graham, K. R.; Amassian, A.; Ade, H.; Fréchet, J. M. J.; Toney, M. F.; McGehee, M. D. *Adv. Energy Mater* **2013**, *3*, 364.

(11) Ma, W. L.; Yang, C. Y.; Gong, X.; Lee, K.; Heeger, A. J. *Adv. Funct. Mater.* **2005**, *15*, 1617.

(12) Li, L.; Lu, G. H.; Yang, X. *J. Mater. Chem.* **2008**, *18*, 1984.

(13) (a) Hou, J. H.; Chen, H. Y.; Zhang, S. Q.; Li, G.; Yang, Y. *J. Am. Chem. Soc.* **2008**, *130*, 16144. (b) Collins, B. A.; Li, Z.; McNeill, C. R.; Ade, H. *Macromolecules* **2011**, *44*, 9747.

(14) Peet, J.; Kim, J. Y.; Coates, N. E.; Ma, W. L.; Moses, D.; Heeger, A. J.; Bazan, G. C. *Nat. Mater.* **2007**, *6*, 497.

(15) Cates, N. C.; Gysel, R.; Beiley, Z.; Miller, C. E.; Toney, M. F.; Heeney, M.; McCulloch, L.; McGehee, M. D. *Nano Lett.* **2009**, *9*, 4153.

(16) (a) Qian, D. P.; Ye, L.; Zhang, M. J.; Liang, Y. R.; Li, L. J.; Huang, Y.; Guo, X.; Zhang, S. Q.; Tan, Z. A.; Hou, J. H. *Macromolecules* **2012**, *45*, 9611. (b) Ie, Y.; Huang, J.; Uetani, Y.; Karakawa, M.; Aso, Y. *Macromolecules* **2012**, *45*, 4564.

(17) Li, Y. F.; Cao, Y.; Gao, J.; Wang, D. L.; Yu, G.; Heeger, A. J. *Synth. Met.* **1999**, *99*, 243.

(18) (a) Sun, Q. J.; Wang, H. Q.; Yang, C. H.; Li, Y. F. *J. Mater. Chem.* **2003**, *13*, 800. (b) Hou, J. H.; Tan, Z. A.; Yan, Y.; He, Y. J.; Yang, C. H.; Li, Y. F. *J. Am. Chem. Soc.* **2006**, *128*, 4911.

(19) Lee, J. K.; Ma, W. L.; Brabec, C. J.; Yuen, J.; Moon, J. S.; Kim, J. Y.; Lee, K.; Bazan, G. C.; Heeger, A. J. *J. Am. Chem. Soc.* **2008**, *130*, 3619.

(20) Huo, L. J.; Zhang, S. Q.; Guo, X.; Xu, F.; Li, Y. F.; Hou, J. H. *Angew. Chem., Int. Ed.* **2011**, *50*, 9697.

(21) Dou, L.; Gao, J.; Richard, E.; You, J.; Chen, C. C.; Cha, K. C.; He, Y. J.; Li, G.; Yang, Y. *J. Am. Chem. Soc.* **2012**, *134*, 10071.

(22) Hoppe, H.; Sariciftci, N. S. *J. Mater. Chem.* **2006**, *16*, 45.

(23) Chen, L. M.; Hong, Z. R.; Li, G.; Yang, Y. *Adv. Mater.* **2009**, *21*, 1434.

(24) Dennler, G.; Scharber, M. C.; Brabec, C. J. *Adv. Mater.* **2009**, *21*, 1323.

(25) Blom, P. W. M.; Mihailetchi, V. D.; Koster, L. J. A.; Markov, D. E. *Adv. Mater.* **2007**, *19*, 1551.

(26) Huang, Y. C.; Tsao, C. S.; Chuang, C. M.; Lee, C. H.; Hsu, F. H.; Cha, H. C.; Chen, C. Y.; Lin, T. H.; Su, C. J.; Jeng, U. S.; Su, W. F. *J. Phys. Chem. C* **2012**, *116*, 10238.

(27) Collins, B. A.; Li, Z.; Tumbleston, J. R.; Gann, E.; McNeill, C. R.; Ade, H. *Adv. Energy Mater.* **2013**, *3*, 65.

(28) Lu, X.; Hlaing, H.; Germack, D. S.; Peet, J.; Jo, W. H.; Andrienko, D.; Kremer, K.; Ocko, B. M. *Nat. Commun.* **2012**, *3*, 795.